

Synthesis, Structure, and Structural Dynamics of a Remarkably Crowded Rhodium(I) Dimer: $[\text{Rh}_2((\text{Me}_2\text{PCH}_2)_2\text{PMe})_2(\text{CO})_2][\text{B}(\text{C}_6\text{H}_5)_4]_2$

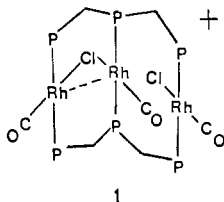
Alan L. Balch,* Marilyn M. Olmstead, and Douglas E. Oram

Received May 30, 1985

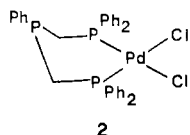
Treatment of a methanol solution of $\text{Rh}_2(\text{CO})_4(\mu\text{-Cl})_2$ with bis((dimethylphosphino)methyl)methylphosphine, dmmm, in dichloromethane followed by precipitation with sodium tetraphenylborate yields yellow $[\text{Rh}_2(\mu\text{-dmmm})_2(\text{CO})_2][\text{BPh}_4]_2$. The structure of this salt has been determined by X-ray crystallography. It crystallizes from acetone/ethyl ether in the orthorhombic space group $Pn2_1m$ (*bca* of No. 31) with 2 molecules/unit cell of dimensions $a = 11.590$ (2), $b = 12.516$ (2), and $c = 22.329$ (4) Å at 140 K. Least-squares refinement of 213 parameters using 2845 reflections yielded $R = 0.057$. The structure of the cation consists of a four-coordinate rhodium (terminal CO, two $\text{CH}_2\text{P}(\text{CH}_3)_2$, and the other Rh as ligands) connected to a six-coordinate rhodium (terminal CO, four $\text{CH}_2\text{P}(\text{CH}_3)_2$, and the other Rh as ligands) through a dative Rh-Rh bond, which is 2.777 (1) Å long. The coordination about the six-coordinate rhodium is distorted so that one trans P-Rh-P unit is nearly linear (173.9 (2)°) and the other is decidedly bent (146.1 (2)°). This distortion is caused by the packing of the methyl and methylene carbons around the OC-Rh-Rh-CO unit. The ^{31}P NMR spectrum is temperature-dependent. In acetone solution at -75 °C the three phosphorus environments are clearly resolved while warming causes broadening and approach to coalescence of the two terminal phosphorus resonances. This behavior is ascribed to a dynamic process that interchanges the PMe_2 groups between the bent and linear environments. In part the barrier to this process results from the packing of the methyl and methylene groups into two nearly planar layers of six groups, which form belts around the OC-Rh-Rh-CO unit.

Introduction

The use of polyfunctional phosphine ligands to construct and stabilize polynuclear transition-metal complexes has undergone significant development in recent years.^{1,2} These ligands generally behave as unreactive connectors that can accommodate reactions at the metal centers while allowing considerable variation in the metal-metal interaction. Recently we have described the coordination properties of the small-bite, linear triphosphine, bis((diphenylphosphino)methyl)phenylphosphine (dpmp).³⁻¹⁰ With $\text{Rh}_2(\text{CO})_4(\mu\text{-Cl})_2$ this ligand produces the nearly linear cation **1**,

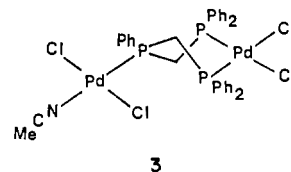


which undergoes a variety of chemical transformations that affect the coordination in the plane perpendicular to the Rh_2P_6 core.^{3,4} This ligand can also act as a chelating ligand by forming six-membered chelate rings that leave the internal phosphorus atom uncoordinated. For example, the reaction between $\text{Pd}(\text{PhCN})_2\text{Cl}_2$ and dpmp produces **2**.⁵ The presence of the phosphorus lone pair



in chelated complexes such as **2** enables them to act as ligands themselves. Thus they can be used to construct both hetero and homo di- and trinuclear complexes.⁹ In these, the chelate ring

generally adopts a skew boat conformation, which places the metal ions in remote locations. As an example, **2** reacts with $(\text{PhCN})_2\text{PdCl}_2$ to form (after recrystallization from acetonitrile) **3**, which has Pd...Pd separation of 5.85 Å.



In pursuit of clusters with more reactive metal centers, we have begun to investigate the properties of the methyl analogue of dpmp. This ligand, bis((dimethylphosphino)methyl)methylphosphine (dmmm), has been previously prepared.¹¹ The higher basicity of the alkylphosphines should allow for the preparation of complexes with more electron rich metal centers. Additionally, the smaller size of the methyl substituents should cause less steric interference to reactions at the metal center. In fact, the effect of steric hindrance of the phenyl rings in binuclear complexes has been a matter of concern to a number of research groups.¹²⁻¹⁴ Here, however, we report that the reaction of dmmm with $\text{Rh}_2(\text{CO})_4(\mu\text{-Cl})_2$ produces a remarkably crowded binuclear complex of a structural type that is unprecedented among the numerous binuclear, phosphine-bridged rhodium(I) complexes.

Results

Synthesis. Treatment of a methanol solution of $\text{Rh}_2(\text{CO})_4(\mu\text{-Cl})_2$ with a dichloromethane solution of dmmm produces a deep purple solution, which yields yellow crystals of $[\text{Rh}_2(\mu\text{-dmmm})_2(\text{CO})_2][\text{BPh}_4]_2$ after the addition of sodium tetraphenylborate. The purple color of the reaction is caused by the presence of $[\text{Rh}_3(\mu\text{-dmmm})_2(\text{CO})_3(\mu\text{-Cl})\text{Cl}]^+$, a trinuclear species related to **1**. The structure and reaction chemistry of this trinuclear compound will be reported separately. Its intense color masks the presence of yellow $[\text{Rh}_2(\mu\text{-dmmm})_2(\text{CO})_2]^{2+}$, which is actually the major product (isolated yield 76%). The infrared spectrum reveals the presence of only terminal carbonyl ligands ($\nu(\text{CO}) = 2031, 1982 \text{ cm}^{-1}$).

Structure of the Cation As Determined by X-ray Crystallography. The salt crystallizes with one tetraphenylborate, half of the complex cation, and half of an acetone molecule in the asymmetric unit. There is disorder present in the cations. As a consequence,

- Balch, A. L. In "Homogeneous Catalysis with Metal Phosphine Complexes"; Pignolet, L. H., Ed.; Plenum Press: New York, 1983; p 167.
- Puddephatt, R. J. *Chem. Soc. Rev.* **1983**, 99.
- Guimerans, R. R.; Olmstead, M. M.; Balch, A. L. *J. Am. Chem. Soc.* **1983**, *105*, 1677.
- Olmstead, M. M.; Guimerans, R. R.; Balch, A. L. *Inorg. Chem.* **1983**, *22*, 2474.
- Olmstead, M. M.; Guimerans, R. R.; Farr, J. P.; Balch, A. L. *Inorg. Chim. Acta.* **1983**, *75*, 199.
- Balch, A. L.; Guimerans, R. R.; Olmstead, M. M. *J. Organomet. Chem.* **1984**, *268*, C38.
- Balch, A. L.; Olmstead, M. M.; Guimerans, R. R. *Inorg. Chim. Acta.* **1984**, *84*, 621.
- Balch, A. L.; Guimerans, R. R.; Linehan, J. *Inorg. Chem.* **1985**, *24*, 290.
- Balch, A. L.; Fossett, L. A.; Guimerans, R. R.; Olmstead, M. M. *Organometallics* **1985**, *4*, 781.
- Balch, A. L.; Olmstead, M. M. *Isr. J. Chem.* **1985**, *25*, 189.

- Karsch, H. H. Z. *Naturforsch., B: Anorg. Chem., Org. Chem.* **1982**, *B37*, 284.
- Kubiak, C. P.; Eisenberg, R. *J. Am. Chem. Soc.* **1977**, *99*, 6129.
- Manojlovic-Muir, L.; Muir, K. W.; Frew, A. A.; Ling, S. S. M.; Thomson, M. A.; Puddephatt, R. *J. Organometallics* **1984**, *3*, 1637.
- King, R. B.; Raghuveer, K. S. *Inorg. Chem.* **1984**, *23*, 2482.

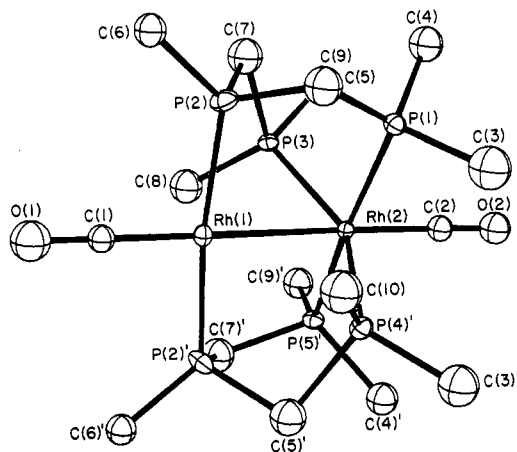


Figure 1. Perspective drawing of $[\text{Rh}_2(\mu\text{-dmmm})_2(\text{CO})_2]^{2+}$ showing the numbering scheme.

although the cations lie on a mirror plane in the crystal, the idealized symmetry of any individual cation is C_2 . We will begin by discussing the geometry of the cation and will then go on to describe how these cations are packed to give the disordered structure. A perspective drawing of the cation is shown in Figure 1. Figure 2 shows a stereoscopic view. Figure 3 shows the relationship of the two disordered forms of the cation.

The cation is built about a nearly linear OC-Rh-Rh-CO unit. The largest deviation from 180° of the angles about any atom in the chain is the Rh(1)-Rh(2)-C(2) angle of $176.8(4)^\circ$. The two triphosphine ligands are connected to this chain so that the central phosphorus atoms are bound in trans fashion to Rh(1). The two terminal phosphorus atoms of each dmmmm are bound to Rh(2). As a result Rh(1) is four-coordinate while Rh(2) is six-coordinate. Because of the way the phosphine ligands are twisted about the $\text{Rh}_2(\text{CO})_2$ chain, the cation has only approximate C_2 symmetry with the symmetry axis lying along the $\text{Rh}_2(\text{CO})_2$ chain. A view of the two enantiomers down this axis is presented at the top of Figure 3.

There is a striking irregularity in the coordination environment of the six-coordinate Rh(2). Although there are four nominally equivalent PMe_2 groups bound to Rh(2), they are sorted out into two distinct sets, which are best categorized by the trans P-Rh-P angles. Thus the two PMe_2 groups involving P(1) and P(5)' are normal coordination sites with a trans angle ($173.9(2)^\circ$) that is nearly linear. For the PMe_2 groups involving P(3) and P(4)', however, the trans P-Rh-P angle ($146.1(2)^\circ$) is sharply bent. The direction of this bend places P(3) and P(4)' closer to Rh(1). As a result the Rh(1)-Rh(2)-P(3) and Rh(1)-Rh(2)-P(4)' angles ($73.3(1)$ and $72.8(1)^\circ$) are less than the ideal 90° while the C(2)-Rh(2)-P(3) and C(2)-Rh(2)-P(4)' angles ($109.9(4)^\circ$ and $104.0(4)^\circ$) are greater. In contrast the corresponding angles involving P(1) and P(5)' fall into the narrow range $86.4\text{--}94.0^\circ$. The direction of the very slight bend is reversed so that these two PMe_2 groups are pushed slightly toward the carbonyl group. Thus the P(1)-Rh(2)-C(2) angle is $86.4(2)^\circ$ and the P(5)'-Rh(2)-C(2) angle is $87.7(2)^\circ$. Despite the asymmetry there is no significant variation in the Rh(2)-P distances between the two sets.

The coordination geometry at Rh(1) is planar and fairly regular. The trans P(2)-Rh(1)-P(2)' angle ($171.2(1)^\circ$) is slightly bent toward Rh(2). Consequently the P(2)-Rh(1)-Rh(2) angle is closed to $85.6(1)^\circ$ while the P(2)-Rh(1)-C(1) angle has opened to $94.4(1)^\circ$. The P-Rh and C-Rh distances are significantly shorter at four-coordinate Rh(1) than the corresponding distances at the six-coordinate Rh(2).

There is a Rh-Rh single bond. The Rh(1)-Rh(2) distance, $2.777(1)\text{ \AA}$, falls into the range of distances found for Rh-Rh single bonds in compounds such as $\text{Rh}_2(\mu\text{-Ph}_2\text{PCH}_2\text{PPh}_2)_2(\text{CO})(\text{o-O}_2\text{C}_6\text{Cl}_4)$ ($2.637(1)\text{ \AA}$),¹⁵ $\text{Rh}_2(\text{p-CH}_3\text{C}_6\text{H}_4\text{NC})_8\text{I}_2^{2+}$

($2.785(1)\text{ \AA}$),¹⁶ $\text{Rh}_2(\mu\text{-CN}(\text{CH}_2)_3\text{NC})_4\text{Cl}_2^{2+}$ ($2.837(1)\text{ \AA}$).¹⁷

The cation has a globular external shape with its surface covered by the methyl and methylene groups of dmmmm and by the oxygens of the two carbonyl groups. The carbon atoms of methyl and methylene groups are particularly tightly packed in two nearly hexagonal layers that lie perpendicular to the $\text{Rh}_2(\text{CO})_2$ axis. One layer (layer A) consists of the methylene carbons C(5), C(5)', C(7), and C(7)' and the methyl carbons C(8) and C(10), which are part of the PMe_2 groups that fall into the bent set. The other layer (layer B) consists of the methyl carbons C(3), C(4), C(4)', and C(9)' of the PMe_2 groups, which fall into the nearly linear set, and the methyl carbons C(9) and C(3)' of the PMe_2 groups in the bent set. A drawing that emphasizes these layers is shown in Figure 4. This drawing gives the deviation of each atom from the least-squares plane of each layer as well as the nonbonded distances between carbon atoms within each of the two layers. Layer A is very nearly planar with C(10) possessing the largest out-of-plane displacement, 0.16 \AA . Within this layer the C...C separations range from 2.88 to 3.28 \AA . These are all considerably less than the sum of the van der Waals radii for two methyl groups (4.0 \AA) so they must reflect tight packing of these groups. The hydrogen atoms probably are arranged in cogwheel fashion to allow this packing. Unfortunately, because of the disorder in the structure, it has not been feasible to locate these hydrogens. Layer B has a somewhat looser structure. It is not nearly so planar; four carbon atoms lie 0.14 \AA on one side of the mean plane while two lie 0.28 \AA on the other side. While the C...C contacts within this layer are all somewhat larger than those in layer A, they are all less than 4 \AA .

The Disorder. The disorder principally involves the phosphorus atoms. The atoms of the $\text{Rh}_2(\text{CO})_2$ chain lie in special positions that are common to both of the two mirror image forms of the cation. One phosphorus atom, P(2), is ordered while the other four, P(1), P(3), P(4), and P(5), represent sites that are occupied by half of a phosphorus atom. These are connected in two different ways to a common set of peripheral carbon atoms that are incorporated into the methyl and methylene groups of the ligands. The cation described in the preceding section and its mirror image are shown side by side at the top of Figure 3. These two forms crystallize together in a 1:1 mixture at a single site in the salt and give rise to the crystallographic mirror plane. The relationship between the two superimposed forms is shown in the lower part of Figure 3. In this drawing form A (on the left side of the top pair) is shown in solid lines while the alternative set of connections to the other placement of phosphorus atoms is shown as open lines. Both forms share many common atoms including all of the carbon atoms, the rhodium atoms, the oxygen atoms and two, P(2) and P(2)', of the phosphorus atoms. However within this unit there are eight phosphorus atom positions, which we have sorted into two sets: site A uses P(1), P(3), P(4)', and P(5)' while site B uses P(1)', P(3)', P(4), and P(5).

Arrangements A and B have very similar external shapes. Consequently the forces involved in the crystallizing process cannot discriminate between them, and they can both occupy the same crystallographic site. The four disordered phosphorus atoms, P(1), P(3), P(4) and P(5), are buried within the cation and have minor influence on the external shape of the cation.

Because of the disorder some of the P-C bonds appear to be unusually long. Generally P-C bonds lengths of this type fall in the range $1.8\text{--}1.9\text{ \AA}$.¹³ However, in the dication there are many P-C distances in the $1.9\text{--}2.0\text{ \AA}$ range. These long bonds all involve carbon atoms that play two roles in the two superimposed forms. In our model these are represented by single carbon atoms, but in reality there may be two closely spaced positions for the two forms that are not resolved by X-ray crystallography. The P(2)-C bonds, which do not have this problem, all fall within the normal range.

(16) Olmstead, M. M.; Balch, A. L. *J. Organomet. Chem.* **1978**, *148*, C15.

(17) Mann, K. R.; Bell, R. A.; Gray, H. B. *Inorg. Chem.* **1980**, *18*, 2671.

(18) Pauling, L. "The Nature of the Chemical Bond", 3rd ed.; Cornell University Press: Ithaca, NY, 1960; p 260.

(15) Ladd, J. A.; Olmstead, M. M.; Balch, A. L. *Inorg. Chem.* **1984**, *23*, 2318.

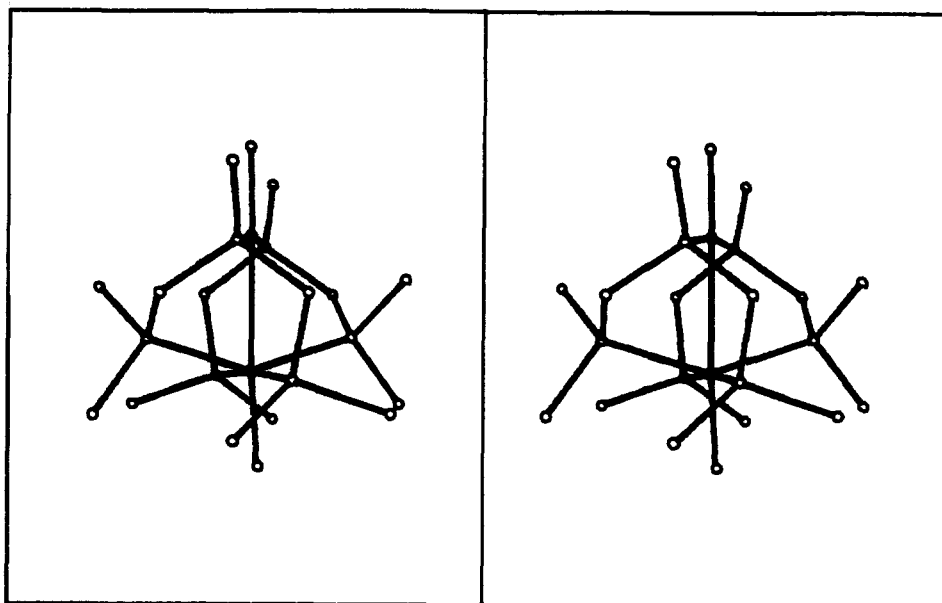


Figure 2. Stereoscopic drawing of $[\text{Rh}_2(\mu\text{-dmmm})_2(\text{CO})_2]^{2+}$.

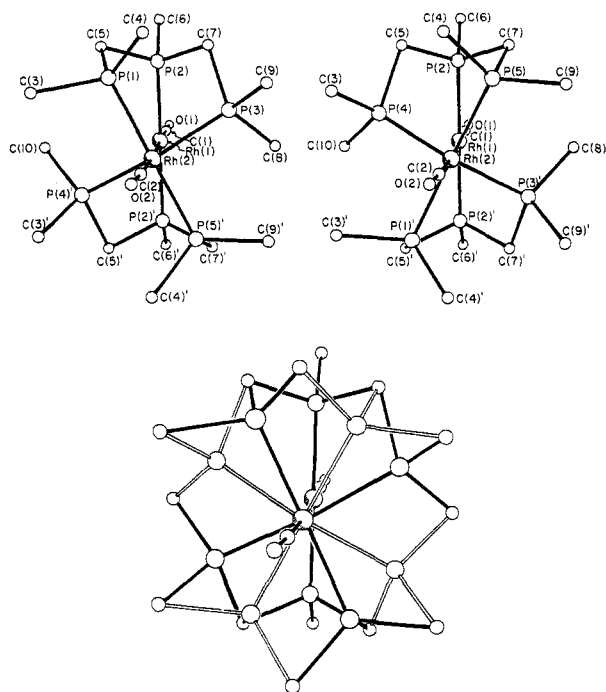


Figure 3. Top: drawings of the mirror images of $[\text{Rh}_2(\text{dmmm})_2(\text{CO})_2]^{2+}$. Bottom: composite drawing showing the superposition of the two forms.

Stereodynamic Behavior As Shown by the ^{31}P NMR Spectrum. The ^{31}P NMR spectra of the dication at -75 and 23°C are shown in traces A and B, respectively, of Figure 5. At -75°C the spectrum shows the presence of three inequivalent phosphorus atoms. Thus the low-temperature spectrum is consistent with the solid-state structure. On warming, two of the resonances broaden as shown in trace B while the third remains sharp with well-resolved coupling. This behavior is fully reversible with temperature. The broadened resonances can be assigned to the terminal PMe_2 groups while the resolved resonance at -3.2 ppm is due to the internal PMe group. The dynamic process must involve interconversion of the PMe_2 groups between the bent and linear set and results in the interconversion of the two enantiomers. This process must be accompanied by the movement of methyl groups between the two layers shown in Figure 3. Thus C(8) and C(10)' must move from layer A to layer B while a methyl group on P(1), and a second methyl group on P(5)' must move from layer B to layer A.

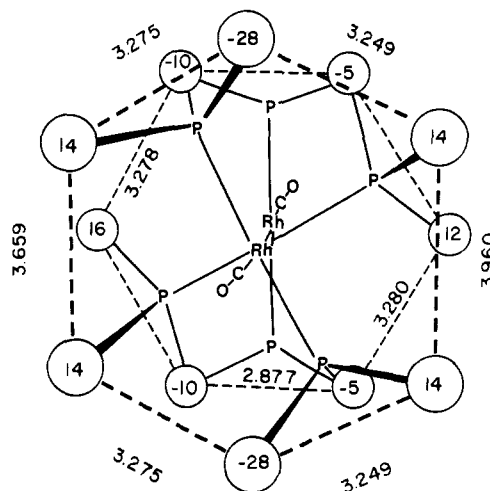


Figure 4. Drawing emphasizing the packing of the methyl and methylene groups into hexagonal layers in $[\text{Rh}_2(\mu\text{-dmmm})_2(\text{CO})_2]^{2+}$. Layer A is shown with small circles denoting carbon atoms, while the carbon atoms of layer B are shown as large circles. The numbers inside each circle give the vertical displacement of each carbon from the least-squares plane of each layer in units of 0.01 \AA . The numbers around the periphery give the nonbridged carbon-carbon separations in layer B. In layer A the separations starting at the top and proceeding clockwise are 2.877 , 3.249 , 3.280 , 2.877 , 3.278 , and 3.275 \AA . The esd in C...C separations is 0.016 \AA .

Although this process should be mirrored in the ^1H NMR spectrum, the observed resolution in the ^1H spectra is insufficient to reveal further information about the process.

Discussion

The cation possesses a number of novel features. The mode of bridging found for the dmmmm ligand is, so far, unique for small-bite triphosphines. The triphosphine forms a six-membered chelate ring about Rh(2) through the use of the terminal PMe_2 groups. The central phosphorus forms the bond to Rh(1). The chelate ring conformation may be described by using the systematic nomenclature developed for propylene diamine chelate rings¹⁹ except that the two NH_2 groups are replaced by PMe_2 groups and the central CH_2 group is replaced by a PMe group. The chelate rings in $[\text{Rh}_2(\text{dmmm})_2(\text{CO})_2]^{2+}$ have adopted the asymmetric boat conformation 4. This conformation exists in two

(19) Hawkins, C. J. "Absolute Configuration of Metal Complexes"; Wiley-Interscience: New York, 1971; pp 11-13, 86-94.

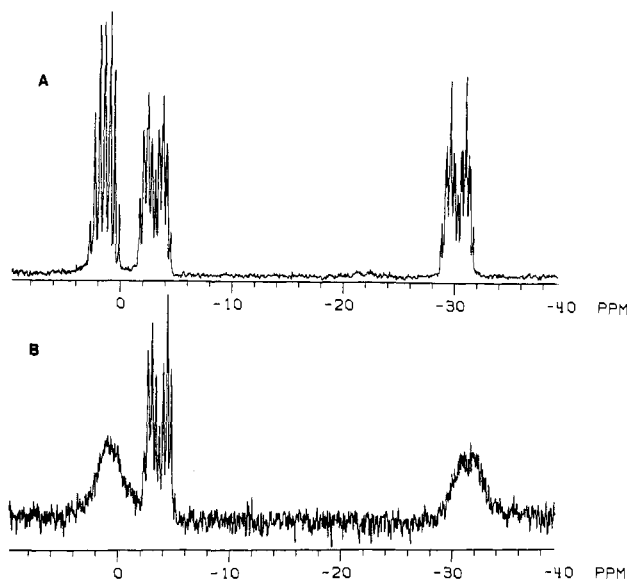
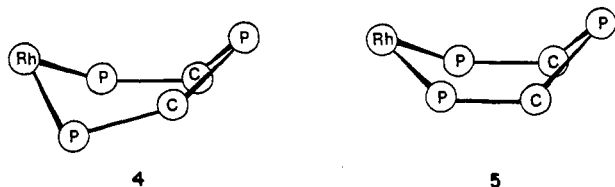


Figure 5. ^{31}P NMR spectrum of $[\text{Rh}_2(\mu\text{-dmmm})_2(\text{CO})_2][\text{BPh}_4]_2$ in acetone- d_6 solution at (A) -75 and (B) 23 °C.

enantiomeric forms, and any one cation contains both rings in the same enantiomeric form.



We had previously noted that the symmetrical boat conformation **5** of this sort of triphosphine ligand should, in principle, be able to hold two metal centers in relatively close proximity.⁵ One can inquire as to why the dication does not utilize the symmetric boat conformation for its chelate rings. A projection down the Rh–Rh axis is shown in Figure 6. The structure has C_{2v} symmetry, and molecular models indicate that the four PMe_2 groups can be equivalent and planar when typical bond distances and angles are used within the dppp ligands. In other words, there are no constraints within the ligand backbone that force a $\text{trans Me}_2\text{P–Rh–PMe}_2$ unit to bend toward the other rhodium. However, two sets of unfavorable methyl–methyl contacts do develop in this model. The separation between the two intraligand pairs of methyl groups labeled *a* is $3.0\text{--}3.5$ Å. More severe contacts exist between the two interligand pairs of methyl groups *b*. The methyl carbons involved lie very near the Rh–P_4 plane, and the separation between them is only $2.0\text{--}2.4$ Å. Both sets of contacts are less than the sum of the van der Waals radii of two methyl groups, 4 Å.¹⁸ In order to alleviate these contacts, the dication twists the chelate rings into the asymmetrical boat conformation by pushing two of the $\text{Rh}(2)\text{–P}$ bonds toward $\text{Rh}(1)$. As a consequence the methyl groups move apart and into the layers shown in Figure 4. Thus the steric effects of the methyl groups produce the distorted environment of $\text{Rh}(2)$. The steric effects of tertiary phosphines are well-known,²⁰ but here relatively small substituents are capable of a major distortion, a distortion comparable to that seen in $\text{RhCl}(\text{PPh}_3)_3$. In this complex, where three bulky triphenylphosphine ligands are involved, a distortion from planarity occurs so that the trans P–Rh–P and P–Rh–Cl angles are 159.1 (2) and 166.7 (2)° in the orange form and 152.8 (1) and 156.2 (2)° in the red form.²¹

The Rh–Rh bond must be a dative single bond with the six-coordinate $\text{Rh}(2)$ acting as a two-electron donor toward $\text{Rh}(1)$. Considering each rhodium as $\text{Rh}(I)$ gives the six-coordinate $\text{Rh}(2)$ an 18-electron count while $\text{Rh}(1)$ is coordinatively unsaturated

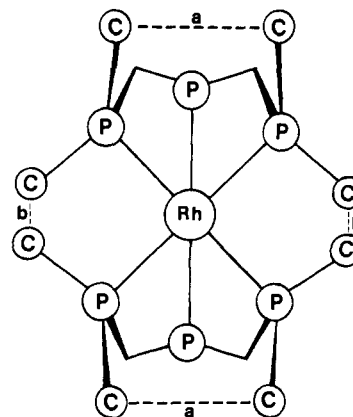
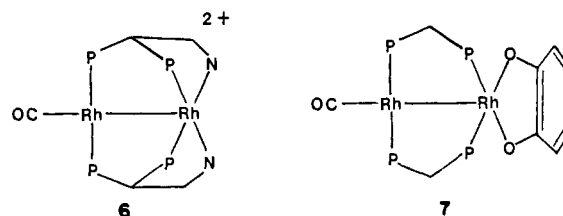


Figure 6. Projection down the RhRh (C_2) axis of the hypothetical structure with both dmmm ligands in symmetric boat conformations. The intra- and interligand methyl–methyl contacts are indicated by *a* and *b*, respectively.

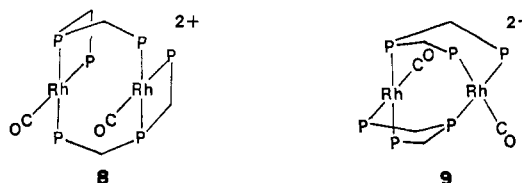
with a 16-electron count. Without the Rh–Rh bond, then, $\text{Rh}(1)$ would only achieve a 14-electron count. The electron imbalance between these two rhodium atoms is further revealed in the bond distances to the ligating atoms. The P–Rh and C–Rh distances at the electron-rich $\text{Rh}(2)$ are all longer than the corresponding distances at $\text{Rh}(1)$.

Two somewhat related dirhodium complexes with Rh–Rh single bonds are known. The dication $[\text{Rh}_2(\text{CO})(\mu\text{-2-pyCH}(\text{PPh}_2)_2)]^{2+}$ (**6**)²² and $\text{Rh}_2(\text{CO})(\mu\text{-O}_2\text{C}_6\text{Cl}_4)(\mu\text{-dpm})_2$ (**7**)²³ both possess



structures in which one rhodium is planar and four-coordinate while the other is five-coordinate. In both cases the Rh–Rh bond distances, 2.674 (1) Å in **6**²² and 2.637 (1) Å in **7**,²³ are shorter than that in $[\text{Rh}_2(\text{dmmm})_2(\text{CO})_2]^{2+}$. Notably, both **6** and **7** lack a carbonyl at one rhodium and consequently achieve only 16-electron counts at each rhodium. In contrast we have not observed any tendency for $[\text{Rh}_2(\text{CO})_2(\text{dmmm})_2]^{2+}$ to lose a carbonyl.

It is worthwhile noting that simpler structures not requiring Rh–Rh bonding could have been constructed with the same constituents found in $[\text{Rh}_2(\mu\text{-dmmm})_2(\text{CO})_2]^{2+}$. A simple monomeric cation $\text{Rh}(\text{CO})(\text{dmmm})^+$ would have the distinct drawback of requiring dmmm to act as a tridentate ligand, which would necessitate the formation of two adjacent four-membered chelate rings. Here ring strain probably prohibits formation. The two face-to-face dimers **8** and **9** are analogous to $\text{Rh}_2(\text{CO})_2\text{Cl}_2(\mu\text{-dpm})_2$.²⁴ Each involves the face-to-face approach of two 16-



electron metal centers; no Rh–Rh bond is required. Complex **8** suffers from the presence of two four-membered chelate rings. Cation **9** suffers from some short methyl–methyl and methyl–methylene contacts in a symmetrical boat chelate ring conformation, but these can be relieved by going to an unsymmetrical boat conformation. This twisting does not require bending of the

(22) Anderson, M. P.; Pignolet, L. H. *Organometallics* **1983**, *2*, 1246.

(23) Ladd, J. A.; Olmstead, M. M.; Balch, A. L. *Inorg. Chem.* **1984**, *23*, 2318.

(24) Cowie, M.; Dwight, S. K. *Inorg. Chem.* **1980**, *19*, 2500.

(20) Tolman, C. A. *Chem. Rev.* **1977**, *77*, 313.

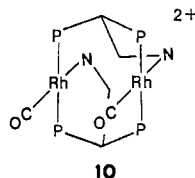
(21) Bennett, M. M.; Donaldson, P. B. *Inorg. Chem.* **1977**, *16*, 655.

Table I. Atom Coordinates ($\times 10^4$) and Temperature Factors ($\text{\AA}^2 \times 10^3$)

atom	x	y	z	U
Rh(1)	2983 (1)	942 (1)	5000	16 (1) ^a
Rh(2)	1900 (1)	2921 (1)	5000	14 (1) ^a
P(1)	1059 (4)	2599 (4)	4054 (2)	21 (1) ^a
P(2)	2917 (2)	1067 (2)	3984 (1)	24 (1) ^a
P(3)	3684 (4)	3146 (4)	4496 (2)	17 (1) ^a
P(4)	652 (4)	1712 (4)	4518 (2)	21 (1) ^a
P(5)	2661 (4)	3424 (4)	4073 (2)	18 (1) ^a
O(1)	4190 (11)	-1154 (10)	5000	54 (3)
O(2)	509 (9)	5036 (9)	5000	46 (3)
O(3)	4802 (29)	1131 (29)	0	217 (14)
C(1)	3715 (11)	-326 (11)	5000	26 (3)
C(2)	1047 (12)	4259 (12)	5000	29 (3)
C(3)	-639 (12)	2384 (12)	4181 (6)	63 (4)
C(4)	1409 (11)	3752 (10)	3522 (5)	48 (3)
C(5)	1417 (11)	1271 (11)	3753 (6)	50 (3)
C(6)	3449 (9)	47 (9)	3498 (5)	35 (2)
C(7)	3630 (11)	2310 (12)	3760 (6)	50 (3)
C(8)	5034 (15)	2842 (17)	5000	53 (4)
C(9)	3827 (10)	4533 (10)	4113 (6)	49 (3)
C(10)	217 (16)	450 (16)	5000	55 (5)
C(11)	7513 (8)	3454 (7)	3033 (4)	23 (2)
C(12)	7033 (8)	3652 (9)	3595 (5)	33 (2)
C(13)	7362 (8)	4515 (8)	3947 (5)	33 (2)
C(14)	8213 (8)	5191 (9)	3781 (5)	32 (2)
C(15)	8679 (9)	5066 (9)	3218 (5)	35 (2)
C(16)	8345 (7)	4229 (8)	2856 (4)	24 (2)
C(17)	7483 (7)	1307 (7)	3040 (4)	22 (2)
C(18)	6841 (8)	1036 (9)	3551 (4)	32 (2)
C(19)	7126 (9)	210 (10)	3923 (5)	42 (3)
C(20)	8072 (9)	-448 (10)	3787 (5)	44 (3)
C(21)	8694 (9)	-207 (8)	3283 (4)	33 (2)
C(22)	8408 (8)	628 (8)	2917 (4)	26 (2)
C(23)	7830 (7)	2346 (8)	1988 (4)	22 (2)
C(24)	9048 (8)	2408 (8)	1954 (4)	29 (2)
C(25)	9619 (9)	2390 (8)	1424 (4)	34 (2)
C(26)	9065 (10)	2281 (10)	900 (5)	46 (3)
C(27)	7847 (10)	2247 (11)	895 (6)	51 (3)
C(28)	7252 (9)	2252 (9)	1442 (4)	35 (2)
C(29)	5748 (7)	2413 (7)	2502 (4)	16 (2)
C(30)	5110 (7)	3362 (7)	2481 (4)	16 (2)
C(31)	3960 (8)	3388 (8)	2297 (4)	26 (2)
C(32)	3415 (9)	2471 (8)	2135 (4)	30 (2)
C(33)	4008 (8)	1498 (8)	2157 (4)	26 (2)
C(34)	5159 (7)	1483 (8)	2348 (4)	23 (2)
C(35)	4081 (25)	1896 (24)	0	100 (9)
C(36)	3895 (18)	2225 (19)	622 (9)	113 (7)
B	7150 (9)	2400 (9)	2637 (5)	22 (2)

^aEquivalent isotropic *U* defined as one-third of the trace of the orthogonalized U_{ij} tensor.

Rh-P bonds. However both structures **8** and **9** as well as the monomeric $\text{Rh}(\text{CO})(\text{dppp})^+$ have a carbonyl ligand trans to a phosphine. This is a grouping that is generally avoided in Rh(I) compounds.²⁵ As an example, $[\text{Rh}_2(\text{CO})_2(\mu\text{-}2\text{-pyCH}(\text{PPh}_2)_2)_2]^{2+}$ (**10**), which has a structure analogous to that of **9**, has the carbonyl group trans to nitrogen rather than trans to phosphorus.²⁶



Experimental Section

The ligand *dmmm* was prepared as described previously.¹¹

Preparation of $[\text{Rh}_2(\mu\text{-}dmmm)_2(\text{CO})_2][\text{BPh}_4]_2$. Under a dioxygen-free environment a solution of *dmmm* (202 mg, 1.03 mmol) in 15 mL of dichloromethane was rapidly added to a stirred solution of $[\text{Rh}(\text{CO})_2\text{Cl}]_2$

Table II. Selected Interatomic Distances (\AA) in $[\text{Rh}_2(\text{dmmm})_2(\text{CO})_2]^{2+}$

Rh(1) Environment			
Rh(1)-P(2)	2.275 (2)	Rh(1)-C(1)	1.799 (14)
Rh(1)-Rh(2)	2.777 (1)	C(1)-O(1)	1.17 (2)
Rh(2) Environment			
Rh(2)-P(1)	2.362 (5)	Rh(2)-P(3)	2.371 (4)
Rh(2)-P(4)'	2.353 (5)	Rh(2)-P(5)'	2.337 (4)
Rh(2)-C(2)	1.945 (14)	C(2)-O(2)	1.16 (2)
Rh(2)-Rh(1)	2.777 (1)		
Phosphine Ligand			
P(1)-C(3)	2.01 (1)	P(2)-C(5)	1.83 (1)
P(1)-C(4)	1.91 (1)	P(2)-C(6)	1.79 (1)
P(1)-C(5)	1.84 (1)	P(2)-C(7)	1.83 (1)
P(3)-C(7)	1.95 (1)	P(4)-C(3)'	1.88 (15)
P(3)-C(8)	1.96 (1)	P(4)-C(5)'	2.00 (1)
P(3)-C(9)	1.94 (1)	P(4)-C(10)	1.98 (2)
P(5)-C(4)'	1.95 (1)	P(5)-C(9)'	1.93 (1)
P(5)-C(7)'	1.92 (1)		

Table III. Selected Interatomic Angles (deg) for $[\text{Rh}_2(\text{dmmm})_2(\text{CO})_2]^{2+}$

At Rh(1)			
P(2)-Rh(1)-Rh(2)	85.6 (1)	P(2)-Rh(1)-C(1)	94.4 (1)
P(2)-Rh(1)-P(2)'	171.2 (1)	Rh(2)-Rh(1)-C(1)	178.7 (4)
Rh(1)-C(1)-O(1)	180.0 (12)		
At Rh(2)			
P(3)-Rh(2)-P(4)'	146.1 (2)	P(1)-Rh(2)-P(5)'	173.9 (2)
P(1)-Rh(2)-P(3)	87.5 (1)	P(1)-Rh(2)-P(4)'	92.6 (2)
P(5)'-Rh(2)-P(3)	93.4 (2)	P(5)'-Rh(2)-P(4)'	90.0 (2)
C(2)-Rh(2)-Rh(1)	176.3 (4)	C(2)-Rh(2)-P(1)	86.4 (2)
C(2)-Rh(2)-P(3)	109.9 (4)	C(2)-Rh(2)-P(4)'	104.0 (4)
C(2)-Rh(2)-P(5)'	87.7 (2)	Rh(1)-Rh(2)-P(1)	92.0 (1)
Rh(1)-Rh(2)-P(3)	73.3 (1)	Rh(1)-Rh(2)-P(4)'	72.8 (1)
Rh(1)-Rh(2)-P(5)'	94.0 (1)	Rh(2)-C(2)-O(2)	177.9 (12)
At Phosphorus			
C(3)-P(1)-C(4)	113.4 (6)	C(4)-P(1)-C(5)	114.0 (6)
C(3)-P(1)-C(5)	98.7 (5)	C(5)-P(2)-C(7)	103.5 (6)
C(5)-P(2)-C(6)	104.8 (5)	C(7)-P(2)-C(6)	106.6 (5)
C(7)-P(3)-C(8)	113.8 (6)	C(7)-P(3)-C(9)	96.4 (6)
C(8)-P(3)-C(9)	110.9 (7)	C(3)'-P(4)'-C(10)	111.9 (7)
C(3)'-P(4)'-C(5)	97.7 (6)	C(10)-P(4)'-C(5)'	110.9 (7)
C(4)'-P(5)'-C(9)'	113.5 (6)	C(4)'-P(5)'-C(7)'	111.0 (6)
C(9)'-P(5)'-C(7)'	97.4 (6)		
At Methylene Carbons			
P(1)-C(5)-P(2)	103.7 (7)	P(2)-C(7)-P(3)	103.9 (6)

(300 mg, 0.772 mmol) in 30 mL of methanol. The solution immediately turned deep purple, and the liberation of carbon monoxide was observed. A solution of sodium tetraphenylborate (400 mg, 1.17 mmol) in methanol was added dropwise over a period of 20 min. After the mixture was stirred for an additional 1 h, yellow crystals of $[\text{Rh}_2(\text{dmmm})_2(\text{CO})_2][\text{BPh}_4]_2$ were collected by filtration of the purple solution. The product was recrystallized from an acetone/ether solution to yield 0.515 g (76%) of yellow crystalline product.

X-ray Data Collection. Well-formed yellow crystals were grown by slow diffusion of diethyl ether into an acetone solution of the compound. Data collection was carried out by using a Syntex P₂₁ diffractometer, a graphite monochromator, Mo $K\alpha$ radiation ($\lambda = 0.71069 \text{ \AA}$), with the crystal cooled to 140 K. The crystal selected was a multifaceted pedion of dimensions $0.20 \times 0.25 \times 0.87 \text{ mm}$ and was mounted with its long axis parallel to ϕ of the diffractometer. By the use of standard procedures, the lattice was determined to be orthorhombic *P* with dimensions (based on a least-squares fit of 15 centered reflections in the range $30^\circ < 2\theta < 35^\circ$) of $a = 11.590 (2) \text{ \AA}$, $b = 12.516 (2) \text{ \AA}$, $c = 22.329 (4) \text{ \AA}$, and $V = 3239 (1) \text{ \AA}^3$. A total of 3244 reflections in the range $0^\circ < 2\theta < 50^\circ$ was collected at a scan speed of $20^\circ \text{ min}^{-1}$ (ω scans), using a range of 1° and a 0.8° offset for background counts. No decay in the intensity of the check reflections was observed. Processing of the data and all further crystallographic computing were carried out by using the SHELXTL Version 4, July 1983 package installed on a Data General Eclipse 3/230 computer.

Solution and Refinement of the Structure. On the basis of the observed condition for present reflections, $0kl$, $k + l = 2n$, several space groups

(25) Sanger, A. R. *J. Chem. Soc., Chem. Commun.* **1975**, 893.

(26) Anderson, M. P.; Tso, C. C.; Mattson, B. M.; Pignolet, L. H. *Inorg. Chem.* **1983**, *22*, 3267.

($Pn2_1m$, $Pnm2_1$, and $Pnmm$) were considered for solution of the structure. An examination of the Patterson map yielded a solution for the positions of the two rhodium atoms in $Pn2_1m$, but since the first difference map yielded too many phosphorus atoms, the other space groups were explored and rejected in turn. When we returned to $Pn2_1m$ (bca of No. 31; equivalent positions (x, y, z) , $(x, y, -z)$, $(-x, 1/2 + y, 1/2 - z)$, $(-x, 1/2 + y, 1/2 + z)$) and included the phosphorus atoms in the structure factor calculation, nearly the entire tetraphenylborate group appeared in the difference map. With this encouragement, the remaining details of the structure were revealed by a combination of least-squares refinement and Fourier difference maps. A crystallographic mirror plane passes through the two terminal carbon monoxide ligands and the two rhodium atoms. Therefore one triphosphine ligand is in the asymmetric unit. The central phosphorus atom of this ligand is well-behaved, but two alternate sites exist for the terminal phosphorus atoms. These are occupied in a 1:1 mixture, which, on average, gives rise to the crystallographic mirror plane. An absorption correction was applied:²⁷ $\mu(\text{Mo K}\alpha) = 6.8 \text{ cm}^{-1}$; range of absorption correction factors 1.12-1.31. Atomic scattering

factors and corrections for anomalous dispersion were from common sources.²⁸ Final blocked-cascade least-squares refinement was carried out on 213 parameters using 2845 reflections for which $I > 2\sigma(I)$. The Rh and P atoms were assigned anisotropic thermal parameters. Only those hydrogens not affected by the disordered phosphorus atoms were included. These were refined by using a riding model with C-H distance of 0.96 Å and U_{iso} (bonded C). The two largest peaks on a final difference map were $1.3 \text{ e } \text{Å}^{-3}$, near acetone and between P(1) and P(4). Refinement converged with $R = 0.053$, $R_w = 0.057$, and $w = [\sigma^2(F_o) + 0.0001F_o^2]^{-1}$. Table I gives the atomic coordinates; Tables II and III give selected interatomic distances and angles, respectively.

Acknowledgment. We thank the National Science Foundation, Grant CHE8217954, for financial support.

Registry No. 1, 99595-11-6; $[\text{Rh}_2(\mu\text{-dmmm})_2(\text{CO})_2][\text{BPh}_4]_2 \cdot \text{CH}_3\text{COCH}_3$, 99595-10-5; $\text{Rh}_2(\text{CO})_4(\mu\text{-Cl})_2$, 14523-22-9.

Supplementary Material Available: Tables of anisotropic thermal parameters, calculated hydrogen coordinates, and structure factors (18 pages). Ordering information is given on any current masthead page.

(27) The method obtains an empirical absorption tensor from an expression relating F_o and F_c : Hope, H.; Moezzi, B., Department of Chemistry, University of California, Davis CA, unpublished results.

(28) "International Tables for X-ray Crystallography"; Kynoch Press: Birmingham, England, 1974; Vol. 4.

Contribution from the Department of Chemistry,
University of California, Davis, California 95616

¹H Nuclear Magnetic Resonance Studies of Iron(III) Porphyrin Complexes with Axial Aryl Ligands

Alan L. Balch* and Mark W. Renner

Received September 4, 1985

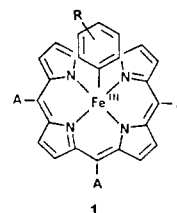
¹H NMR spectra of low-spin ($S = 1/2$) iron(III) tetraarylporphyrin complexes bearing axial phenyl and *o*-, *m*-, and *p*-tolyl groups have been recorded and assigned. Addition of imidazole, 1-methylimidazole, 2-methylimidazole, 1,5-dimethylimidazole, and 1,4-dimethylimidazole to these five-coordinate complexes at -60 °C in chloroform gives six-coordinate adducts. The pattern of aryliron and porphyrin resonances remains the same in both the five- and six-coordinate adducts. Distinct resonances of the coordinated imidazole have been resolved and assigned. Analysis of the hyperfine shifts indicates π spin in the axial aryl groups of both five- and six-coordinate complexes and in the axial imidazole of the six-coordinate complexes. Comparisons of these results are made with the published spectra for the corresponding protein complexes derived from the arylhydrazine/dioxygen reaction with myoglobin. The patterns of resonances for phenyl, *p*-tolyl, and *m*-tolyl complexes are similar, but the model compound for the *o*-tolyl complex does not show the curious doubling of resonances, ascribed previously to restricted rotation, seen for *o*-tolylmyoglobin. Low-field resonances in the 40-20 ppm region of the protein spectra can now be assigned to histidine imidazole (2-H and 4-H) resonances.

Introduction

Iron(III) porphyrin complexes bearing an axial phenyl (or substituted phenyl) ligand have been established as key intermediates in the destruction of heme proteins by arylhydrazines.¹⁻³ Exposure of myoglobin to arylhydrazines in the presence of dioxygen leads to the eventual formation of *N*-arylprotoporphyrin IX.⁴⁻⁶ The iron(III)-aryl intermediates have been directly observed by ¹H NMR spectroscopy.^{1,2} The iron-bound phenyl group displays characteristic paramagnetically shifted resonances, which place the ortho and para resonances upfield at ca. -80 and -20 ppm and the meta resonance downfield at ca. 13 ppm at 25 °C. The three tolyl hydrazines also form corresponding iron-tolyl complexes with heme proteins. However, the *o*-tolyl derivative possesses a distinctly different chromophore⁷⁻¹⁰ and an unusual

¹H NMR spectrum, which shows a doubling of resonances. This doubling has been interpreted to indicate the presence of two noninterconverting isomers.² Moreover the *o*-tolyl complex does not lead to the eventual formation of an *N*-substituted porphyrin.⁶ In addition to extensive characterization by ¹H NMR spectroscopy,^{1,2} phenylmyoglobin has been crystallized and subject to an X-ray diffraction study.³ This study showed that the iron is six-coordinate and bound to the phenyl group and the proximal histidine imidazole as axial ligands.

Corresponding model complexes **1** are available from the reaction of Grignard reagents with iron(III) porphyrin halide complexes.¹¹⁻¹³ One such five-coordinate complex has been



- (1) Kunze, K. L.; Ortiz de Montellano, P. R. *J. Am. Chem. Soc.* **1983**, *105*, 1380.
- (2) Ortiz de Montellano, P. R.; Kerr, D. E. *Biochemistry* **1985**, *24*, 1147.
- (3) Ringe, D.; Petsko, G. A.; Kerr, D. E.; Ortiz de Montellano, P. R. *Biochemistry* **1984**, *23*, 2.
- (4) Saito, S.; Hano, H. A. *Proc. Natl. Acad. Sci. U.S.A.* **1981**, *78*, 5508.
- (5) Ortiz de Montellano, P. R.; Kunze, K. L. *J. Am. Chem. Soc.* **1981**, *103*, 6534.
- (6) Augusto, O.; Kunze, K. L.; Ortiz de Montellano, P. R. *J. Biol. Chem.* **1982**, *257*, 6231.
- (7) Huang, P.-K. C.; Kosower, E. M. *Biochim. Biophys. Acta* **1968**, *165*, 483.
- (8) Itano, H. A. *Proc. Natl. Acad. Sci. U.S.A.* **1970**, *67*, 485.
- (9) Itano, H. A.; Hirota, K.; Hosokawa, K. *Nature (London)* **1975**, *256*, 665.

- (10) Itano, H. A.; Hirota, K.; Vedvick, T. S. *Proc. Natl. Acad. Sci. U.S.A.* **1977**, *74*, 2556.
- (11) Ogoshi, H.; Sugimoto, H.; Yoshida, Z.-I.; Kobayashi, H.; Sakai, H.; Maeda, Y. *J. Organomet. Chem.* **1982**, *234*, 185.
- (12) Coccolios, P.; Laviron, E.; Guillard, R. J. *J. Organomet. Chem.* **1982**, *228*, C39.